Hindawi
International Transactions on Electrical Energy Systems
Volume 2023, Article ID 6614905, 22 pages
https://doi.org/10.1155/2023/6614905

Research Article

Role of Voltage Control Devices in Low Voltage State Estimation Process

István Táczi,[1] **István Vokony**,[1] **Lilla Barancsuk**,[1] **Gábor Mihály Péter**,[2] **Balázs Tőzsér**,[2] **and Bálint Hartmann**[1]

[1]*Department of Electric Power Engineering, Budapest University of Technology and Economics, Budapest H-1111, Hungary*
[2]*Department of Coordination and Innovation, E.ON DSO Hungary, Győr H-9027, Hungary*

Correspondence should be addressed to István Táczi; taczi.istvan@edu.bme.hu

Received 20 March 2023; Revised 3 July 2023; Accepted 17 August 2023; Published 6 September 2023

Academic Editor: Michele De Santis

Copyright © 2023 István Táczi et al. This is an open access article distributed under the Creative Commons Attribution License, which permits unrestricted use, distribution, and reproduction in any medium, provided the original work is properly cited.

Megatrends, such as the proliferation of distributed generation, electrification, and the appearance of aggregator companies, put the low voltage power grids under intense pressure. Since the network infrastructure developments cannot keep up with the trends, distribution system operators turned to alternative solutions. Smart grid assets, such as on-load tap-changing distribution transformers or serial low voltage regulators, are promising solutions. However, the energy transition cannot be handled with the network expansive on the distribution level. Control centers are predicted to expand to this voltage level in the near future, and distribution system state estimation could be an enabler of all functionalities. On the low voltage level, data scarcity is a great challenge in observability; therefore, research must focus on the creation of pseudomeasurements and integration of available data sources. This paper examines the inclusion of smart assets from the conceptual point to the application on two sites, based on data from operational environments, both with a pseudomeasurement and an integrated metering point approach. The results showed that integrating smart assets could considerably mitigate voltage fluctuations, and reduce estimation errors by two magnitudes on the low voltage network.

1. Introduction

Nowadays, continuous change is the only permanent process in the energy industry. Volatile market prices, renewable generation, emerging technology solutions, and many other aspects are influencing the distribution system. In the past, electricity was provided to the consumers mostly from centralized, large power plants. However, this system had its own challenges, such as power losses and reliance on fossil fuels, and thus the contribution to the greenhouse effect [1]. Distributed generators, defined as electricity sources connected directly to the distribution network, have become a solution for the economical supply of consumers with reliable electricity. However, there are many technical challenges in the integration process of these elements. Voltage stability and voltage control are of utmost importance in the integration; and parameters for control should be based on a network calculation. Voltage control may be the most significant technical challenge limiting the penetration of renewable distributed generators into the distribution system. Mahmud and Zahedi [2] reviewed the concept regarding smart distribution networks thoroughly, observing the latest research advancements of voltage control strategies for distribution systems with a high share of renewable distributed generators and offered a brief overview of different control methods. Xu and Taylor [3] provide a comprehensive overview of voltage control techniques for distributed generation-related electrical distribution networks, making recommendations for increasing grid voltage stability and maximizing distributed generation utilization; and prove that it is possible to gain enhanced voltage control capability via state estimation. State estimation is a technique that uses mathematical methods in power systems. It is basically a data processing algorithm that uses measurements and other information sources to create the state of the electric power system: voltage magnitudes and angles on busbars and power flows on branches.

Observability is a key attribute for distribution system operators to identify issues and react accordingly [4]. As for the distribution system, where there are usually lack of measuring units and control devices, the "hardware" should be substituted with "smart solutions." One of these solutions is state estimation, which can enhance the observability and situational awareness on the distribution level. State estimation is currently well-founded at the transmission system level of the electric grid, as this is the field in which the procedure has been applied for decades. It is also currently one of the most important elements of energy management systems used in monitoring, in addition to the control centers of electrical transmission systems [4]. Despite it is wide spread in transmission system monitoring, state estimation has not yet been widely extended to distribution system monitoring, as these network parts have mostly existed passively with unidirectional power flow. This object scenario is currently going through changes: the concept of the smart grid modifies the properties of electrical distribution networks. Distributed generation is spreading, demand-responsive loads emerge, and new types of metering devices are introduced, which can handle multiple data rates. Thus, it is an absolute must to develop a tool for distribution system state estimation (DSSE). Also, innovative technologies are required in order to protect and optimize the system and apply novel control techniques and other functions that are entailed by the smart grid concept [4].

Owing to the different features of distributing electricity from transmission systems, the conventional and industry-ready state estimation solutions cannot be applied to these systems without further research. Creating a sustainable energy environment leads to active distribution networks, where different kind of generation and load are simultaneously present. In setting up appropriate network models in order to make online monitoring and analysis possible, state estimation is a key function [5]. DSSE requirements are becoming increasingly stringent in the modeling process of the emerging new system. The operational methods for integrating distributed energy resources into the grid and the introduction of cutting-edge technologies into the distribution network also require the results of DSSE.

The data source and the measurement information are the key criteria for state estimation applicability. As the amount of measured data increases, the more accurate the estimation result can be. Abdolahi and Kalantari [6] proposed a method to minimize the measurement device numbers in large scale asymmetric distribution networks with an innovative two-stage stochastic programming model.

Unlike transmission systems, distribution systems are sparsely monitored, making estimation challenging. When measurement cannot be deployed due to economic, technical, or other reasons, pseudomeasurements [7] are used to ensure observability. Pseudomeasurement is a key concept in distribution system state estimation: artificially generated datasets are produced in order to substitute actual measurements when there is insufficient information about the network's physical quantities. Pseudomeasurements approximate these unmeasured quantities, and as such, are commonly devised, applying historical datasets and load profiles. In this paper, direct measurements of physical quantities obtained from the network are referred to as "*measurements*." Conversely, pseudomeasurements encompass any input data to the state estimation that is artificially synthesized to approximate nonmeasured physical quantities, e.g., load profiles or known voltage control device set points.

Due to the lack of adequate measurements in distribution systems, state estimation heavily relies on pseudomeasurements; therefore, the accuracy of pseudomeasurements directly impacts the accuracy of state estimation. In recent years, several pseudomeasurement generation techniques have been proposed, aiming to improve accuracy. A framework to estimate the condition of the distribution system based on robust pseudomeasurement modeling is proposed by Cao et al. [7]. Measurement data at the user level were applied to train the gradient boosting tree models to generate pseudomeasurements. In the next step, a ladder iterative state estimator solved the grid equation in the different system states, relying on the output of the previous step.

Branch current estimation methods and algorithms have proven to be effective in comparison to the distribution system model based on classical node voltages [8]. Despite its success, the international literature basically lacks the description of a detailed system model that includes all components, involving transformers and regulators as well. Neto and Asada [9] discussed component modeling and the necessary changes to the composition of an algorithm which includes various transformer and regulator models. Substation voltage estimation is also carried out using the theory of multisensor data fusion, which describes different classes and measurement types. Another approach is the stochastic gradient method [10], which helps the development of new, fast DSSE paradigms relying on the real-time data stream of asynchronous measurements, which are made available by the latest info-communication technology.

Power grid condition assessment, which is based on machine learning, faces serious challenges, as model training requires a lot of time, and local optima are easy to fall into. To solve these issues, Luo et al. [11] proposed a novel broad, learning-based state estimation approach for the power system. Relying on the theory of matrix pseudoinverse, the proposed learning system does not only solve the problem of speed by computing the connection weights between the different network layers at a high pace, but can also learn in an incremental way.

Besides the observability that DSSE offers, it has several more applications, as twenty different use cases prove that the method offers valuable results [12]. Despite that, it seems that theory and practice differ considerably, and most authors aimed to increase accuracy by integrating new measurement and information sources. There are four major application fields [12].

(i) Outage management and power quality
(ii) Data analysis
(iii) Integration of renewables and e-mobility
(iv) Coordinated control

If taking into account economic considerations, pseudodata generation is essential for low voltage (LV) topologies to complement real measuring devices. However, the performance of this novel method is significantly dependent on the structure of the actual grid and the metering point distribution [12].

As a result of the growing penetration of renewable energy sources, operating conditions of distribution systems are becoming more uncertain and volatile. Thus, besides grid state monitoring, the DSSE must also follow the state of renewable energy sources even in unbalanced conditions [13]. A joint state estimation model for unbalanced distribution systems was proposed [13]. The model can handle a system that includes both single-phase and three-phase solar photovoltaic (PV) power plants. Also, an extended weighted least square (WLS) model complements their system. In the view of the problems arising from the insufficiency of real-time measurements in active distribution networks, Cheng et al. [14] created a state estimation method for such grids based on the forecast of PV energy production. First, an extreme learning machine integrated with a genetic algorithm predicts the amount of power generated by the PV cells. Second, forecast error is estimated by the Gaussian mixture model. The forecast value of PV power generation is corrected by the weighted average of the forecast error, while the weighted standard deviation of the forecast error serves as the basis for pseudomeasurement weight setting. In the last step, the WLS algorithm is applied to estimate the state of the active distribution network, using the real-time measurements collected by the supervisory control and data acquisition system, the predicted pseudomeasurements, and the virtual measurements. A dynamic state estimation installed locally in the converter was proposed by Zhang et al. [15]. This method relies on the voltage and current sampling values of the common coupling point and the direct current bus instead of phasors for estimation, in order to reach real-time high accuracy. A mathematical model of the grid-connected converter is proposed for the most typical topology and control strategy.

The main problem with the LV DSSE is the lack of low-error meters implemented in the distribution system. For the characterization of LV loads, usually synthetic load profiles (SLPs) are used, historical data is only available with the smart and automatically read meters (in many countries, including Hungary, the penetration of such meters is rather low). The number of grid meters in the LV network is low, and the installation of more devices is only to be scheduled in the upcoming decade. As a consequence, right now in most of the countries, only the LV pilot projects provide real-time data. For the monitoring of power quality, periodic measurements are applied, but these datasets are usually too small, thus they cannot be used for the development of the grid. The number of real-time datasets is even lower. The installation of smart devices can be used to increase the number of measured points. The number of smart devices is growing in Hungary, and the implementation of hundreds of them can be expected in the following years. These smart solutions have two main purposes, with regard to state estimation.

(i) They lower the variation of the parameters, thus the estimated value of the variables (the voltage magnitude in particular in LV grids) is expected to remain in a smaller range
(ii) They can be used as a data source in state estimation
    (1) If their data are not connected directly to the state estimation, pseudodata can be created from their historical measurements, or in other words, based on their control logic and a few assumptions
    (2) When directly channeled into the state estimation framework, these measurements can increase real-time accuracy

This paper analyses the role of smart, innovative devices in the LV DSSE, with creating a new type of information source (pseudomeasurement or real measurement), and in this way extending the WLS framework. The structure of the paper is as follows. The introduction gives a thorough analysis of international literature, while the second section introduces the mathematical background of the DSSE model; and its connection with the electrical calculations are presented. After that, the modeling considerations, the used measurements, the contribution of smart assets in LV DSSE, and the modeling framework are shown, which were used in the simulation study section. The simulation study section is based on the modeling of two MV/LV sites. To simulate the effect of smart assets, three different scenarios were proposed, each improving the precision of DSSE compared to load flow calculations.

The results of the paper go beyond the state-of-the-art in the effect analysis of the use of voltage control devices that are getting more common in power grids within a DSSE algorithm as a new data source. The control logic of these devices can be used to process historical data, which acts as a constrain in the making of the measurements. Compared to normal historical data, the new pseudomeasurements can decrease the standard deviation (which is defined as the error in this paper) of voltage magnitude values in the LV DSSE process. These error decreasing data similar to the previously mentioned measurements will be even more accessible with the spreading of innovative technologies and the measurements integrated with them. The paper evaluates the actual measurement integration from the devices, which would require communication and information technology investments from the DSOs. It is concluded that the use of innovative tools as a data source in the grid drastically reduces the error when using DSSE, which is important in the process of the LV grid monitoring infrastructure development.

2. DSSE Mathematical Background and Connections with Electrical Calculations

It is worth mentioning some of the aspects from the linear algebraic background that is important from the viewpoint of DSSE and load flow equations, and it also helps to understand in detail the effects of different pseudomeasurement techniques and data sources. A brief reminder is deemed necessary in the area of the applicable matrix equations to illustrate the way state estimation works with some examples. Drawing on two authoritative sources by Monticelli [16] and Strang [17], a discussion is provided below that links mathematical abstraction with engineering applications, thus revealing what is behind the well-known state estimation equations. After outlining the general state estimation equations, the least square approach is described in order to make the state estimation logic more understandable, decoupling form it the load flow equations. It is worth emphasizing that a state estimator has to handle the nonlinearity of the load flow equation, similarly to a load flow approach, but the state estimation is based on the least square approach.

2.1. Concept of State Estimation. Ahmad et al. [4] outlines the framework of the state estimation equation system, in which the base equation is as follows:

$$z = h(x) + e, \tag{1}$$

where z is the measurements vector, e is the observation noise, x is the state variable, and h is the nonlinear vector function relating the measurements to the state variables. This function can be evaluated by solving the power flow equation system, as described by Abur and Exposito [18] as follows:

$$\begin{aligned}
P_i &= V_i \sum_{j=0}^{N} V_j\left(G_{ij}\cos\theta_{ij} + B_{ij}\sin\theta_{ij}\right),\\
Q_i &= V_i \sum_{j=0}^{N} V_j\left(G_{ij}\sin\theta_{ij} - B_{ij}\cos\theta_{ij}\right),\\
P_{ij} &= V_i V_j\left(G_{ij}\cos\theta_{ij} + B_{ij}\sin\theta_{ij}\right) - G_i V_i^2,\\
Q_{ij} &= V_i V_j\left(G_{ij}\sin\theta_{ij} - B_{ij}\cos\theta_{ij}\right) + B_i V_i^2,
\end{aligned} \tag{2}$$

where P and Q are the active and reactive power flowing from the node i to j, while G and B are the real and imaginary part of admittance, respectively. Due to the nonlinear nature of power systems, a linearization process is needed around a given point (operating characteristics) as follows [4]:

$$z = h(x_0) + (x - x_0)\left(\frac{\partial h(x)}{\partial x}\right) + e(x) + h.o.t, \tag{3}$$

where *h.o.t.* is the higher order term and the index zero denotes the initial state. After reordering the equation and neglecting the *h.o.t.* (first-order linearization), the following, widely used formula, can be given as follows [4]:

$$\begin{aligned}
z - h(x_0) &= (x - x_0)\left(\frac{\partial h(x)}{\partial x}\right) + e(x) \longrightarrow \Delta z\\
&= H\Delta x + e(x),
\end{aligned} \tag{4}$$

where H is the Jacobian matrix. Introducing measurement covariance matrix as the vector of variances from all measurements and its inverse W, which is the measurement weight matrix, the gain matrix (G) is defined as follows [4]:

$$G = H^T W H. \tag{5}$$

The WLS method, which is a wide-spread method for state estimation, is based on error minimalization, with the objective function f as follows [4]:

$$\begin{aligned}
\min f &= (z - h(x))\\
&= \min (z - h(x))^T W (z - h(x)).
\end{aligned} \tag{6}$$

State estimation can be obtained by the iterative solution of equation (7). Equation (7) itself is a system of equations which in the practice can be solved by iteration. At iteration k, the solution for the state variable x is given as follows [4]:

$$\Delta x = G^{-1} H^T W (z - h(x)), \tag{7}$$

$$x^{k+1} = x^k + \Delta x^{k+1}. \tag{8}$$

Equation (7) can be derived using equations (4), (5), and (12)–(14). Otherwise equations (12)–(14) give a better understanding of the G matrix, which is used commonly in state estimation literature, frequently without explanation based on linear algebra. The solution process is described with detailed flowcharts in a previous research by Mutanen et al. [19] or Florez et al. [20], which is useful for further understanding. The latter also introduces a new nonlinear programming model to consider that there are errors in the measurement and handles this error as a constraint. Equation (6) defined the minimization problem, meanwhile Monticelli [16] gave a glimpse behind the curtain. The least squares solution provides one way of dealing with overdetermined systems of linear equations (systems with more equations than variables) of the type. The following general equation can be formulated as follows [16]:

$$Ax = b, \tag{9}$$

where x and b are n and m element vectors, respectively, with $n < m$. A is an $m \times n$ matrix. From here, the focus of this discussion switches to linear algebra. The residual r can be defined as follows [16]:

$$r = b - Ax, \tag{10}$$

which is minimalized using the least square approach as follows [16]:

$$\min\left(r^T r\right) = \min\left(J(x) = \frac{1}{2}(b - Ax)^T (b - Ax)\right). \tag{11}$$

At the location of the minimum, all derivatives are zero, which leads to the following equation (16):

$$A^T A\hat{x} = A^T b,$$
$$\hat{x} = \left(A^T A\right)^{-1} A^T b, \tag{12}$$

where $\hat{x}$ itself is the estimated state, an approximation. The following parts can also be defined [16]:

$$\text{Gain matrix} = G = A^T A, \tag{13}$$

$$\text{Pseudo} - \text{inverse of } A = A^I = \left(A^T A\right)^{-1} A^T. \tag{14}$$

In this way, it is becoming clear, that in the above model, A corresponds to H in equation (4), and the gain matrix G corresponds to $A^T A$, respectively. In this formulation, weighting is not applied; therefore, the weight matrix (W) is not present. It is very helpful in practice to weigh the measurements according to their errors, but it is not necessary to introduce W to discuss the mathematical principles of the state estimation.

2.2. Connection with the Electrical Calculation. Observability and controllability are two important terms for future DSSE systems. Observability is strongly connected to the gain matrix: if it is nonsingular, thus invertible, then the network (or any system concerned) is observable, all of the state variables can be estimated [16]. Controllability is connected to the so-called minimum-norm solution, where the A matrix is short and wide, so there are more variables than equations. In this case the underdetermined system can be solved in a least square sense with the following formulation [16]:

$$\hat{x} = A^T\left(AA^T\right)^{-1} b = A^I b. \tag{15}$$

If AA^T is invertible (nonsingular), then the network is controllable. In other words, there are enough control variables to have an impact on controllable variables in the required way. Moreover, the mathematical expression of controllability makes sense to show its close connection with the least square approach and linear algebra.

A system level understanding of the different types of linear equations can be gained from Strang [17]. Furthermore, an overview of the different formulations and their usage in engineering practice is given in Figure 1.

This categorization consists of four types of equations and their corresponding practical problems. The bottom of the figure contains an overview of matrix structures, using the reduced row echelon form of matrix R. This matrix form is very useful for illustrating the shape of matrices in the system of equations. The different types of system equations are further detailed in Table 1.

For Type 1 scenario of system equations and variables, there is only one solution. The number of variables (n) is equal to the number of equations (m). Regarding Type 2, there is an infinite number of solutions, as $m < n$. In the examples given in Table 1, there are three pivot variables and two free variables. The pivot columns represent the independent variables, and the number equals to the rank of matrix. Then, the system is underdetermined. This is where minimum-norm solution or linear programming will be relevant. The hyperplane has an infinite number of solutions, and there are rules to determine which one is appropriate. In the case of Type 3, there is no "official" solution, as there are more equations than variables. The system is overdetermined. This is where the least square solution will be relevant. There are many measurement points which have to be fitted to a line graphically (explanation below). Type 4 has infinite or zero solutions. This is the mixture of least square and minimum-norm solution. It is rare in practice. However, some sources, e.g., [21–24], discuss this type from a mathematical point of view, because the two types of approximation (least square and minimum-norm) are applicable here, but with constraints.

From the above types, Type 2 and Type 3 are further detailed here, as these are the least square solution and the minimum-norm solution, respectively. Since the focus of present article is state estimation, a general overview is given about the minimum-norm solution and the least square solution. Figure 2 gives a general picture about the geometric meaning of the two scenarios.

The left part of the pictures in Figure 2(a) describes the equations where there are more variables (n) than equations (m). The solution can be split into two parts, namely, the particular (x_p) and special solution (x_n) as follows:

$$Ax = b = x_p + x_n. \tag{16}$$

The special solution of $Ax = 0$ is based on free variables. The particular solution is connected to the pivot variables. The pivot variables give the rank of the matrix. There are n-r (or with the number of equations, n-m) special solutions. Figure 3 gives a geometric view about the different solutions.

The left part of Figure 3(a) corresponds to the left part of Figure 4(a). If there are more variables than equations, freedom increases. However, there is a feasible solution, e.g., on a hyperplane, but it is not known where the optimum is. The special solutions give only one way to select a solution. This question leads further to the minimum-norm solution or linear programming. The minimum-norm solution selects one point, e.g., from a hyperplane, i.e., the minimum-norm is the norm of the hyperplane, so the intersection of the vector and the plane defines the point. Meanwhile, linear programs are seeking the optimum, but it is necessary to give some additional rules for this optimum searching.

The right part of both Figures 2 and 3(b) depicts the heart of mathematical basis of state estimation solution with the least squares. For such a matrix, where there are more equations than variables, the description corresponds to the practical problem of power flows, where we have more measurements than state variables. In state estimation, the projection is an approximation, which is the estimation of a state variable (e.g., voltage at a node). Vector b is the

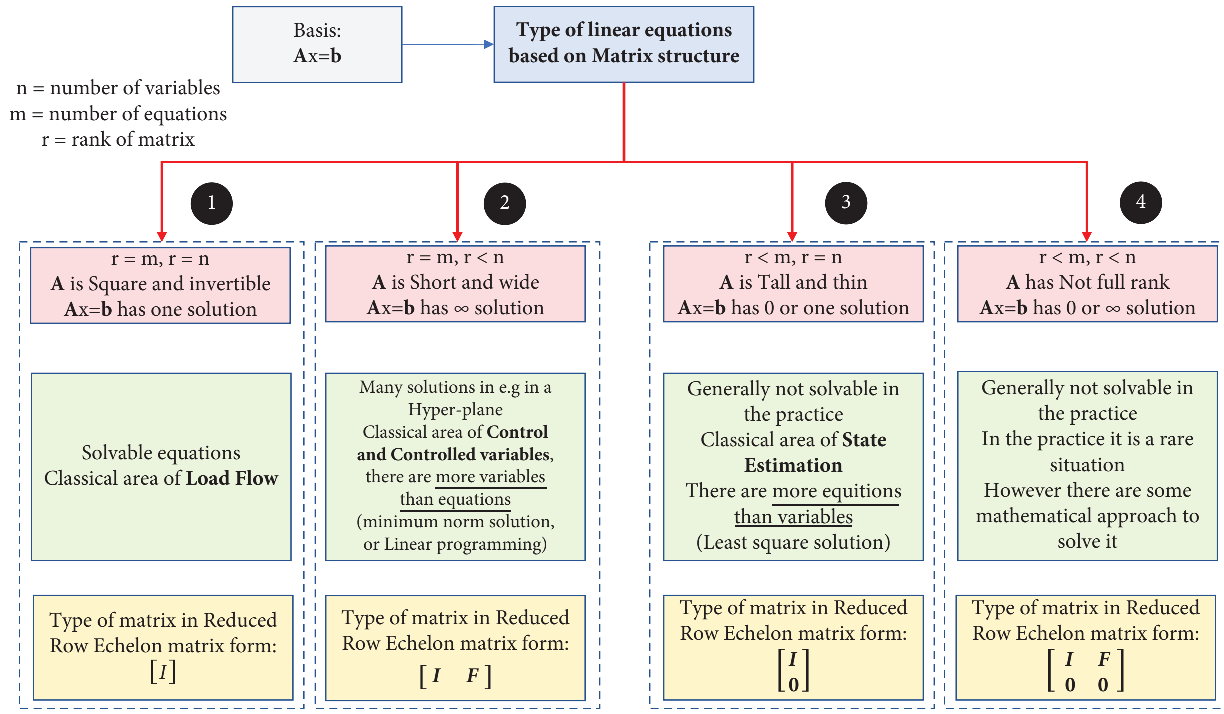

Figure 1: Type of equations, matrices, and relationship to practical problems.

measurement, where we have no solutions; therefore, we are seeking the solution which has the minimum error. This is a projection of vector b to a line. The projection p and the error e (or in other words residual) give vector b. The vector e will have a minimum length if it is orthogonal to a line, so we are seeking such vector e which is orthogonal to a. This will give the minimum error and leads to the least square method. If $e = b - a$, $\hat{x}$ is orthogonal to a, the dot product is zero. It is better to use a^T instead of a because of matrix formulation, so the projection, in the case of state estimation, the estimation itself, is the following; for higher dimensions see equation (15).

$$\hat{x} = \frac{a^T b}{a^T a}. \tag{17}$$

So, there is a system of equations consisting of m equations containing n variables. This can be solved by approximation, similarly to fitting the measurement points to a straight line (with least squares there as well). The basis of the least squares method is the minimization of the residual squares, which means the minimization of the matrix product $r^T r$ as defined in (11). Minimization can be performed by derivation, as the derivative equals to zero or the geometry consideration discussed above. $\hat{x}$ will be the basis of the solution instead of x (x cannot be calculated and $\hat{x}$ is an approximation).

In this way, it is understandable how the additional real or pseudomeasurements work in the process state estimation. The more the measurements, the higher the accuracy of the result (more points to be fitted to a “line”). Naturally, there are different types of measurements, the accuracy of which is varied. Therefore, the engineering practice uses the so-called W measurement weight matrix. Békési et al. [25] improved a state estimation process in which W is used.

If supervisory control and data acquisition (SCADA) measurements and smart metering consumption data are used, they differ from the SLP of consumption, as the former has higher accuracy, so W contains more accurate measurements for state estimation. Furthermore, SCADA measurement means in this context additional data to SLP and automated meter reading so the state estimation can use the advantage provided by the least square. The aim of the future operation of grid control systems is to implement a DSSE framework as accurate as possible. There is an economical constraint as well; therefore, a rational balance is needed between more accurate pseudomeasurements and investment. The so-called smart technologies can give a support for state estimation, because they gather data about the LV grid during operation.

Besides smart grid assets, there are further possibilities to control the system variables. One of them is demand side response, e.g., if a water heating equipment is controlled based on network constraints. This type of problem is leading to the minimum-norm solution and linear programming. In this case, for example, there is one controllable variable (voltage at a node), but there are some equipment (e.g., demand equipment) which means more equations.

3. Methodology

This chapter summarizes the modeling considerations used in the grid calculations. First, the network parameters and load data are discussed, then the smart asset principles are covered.

Table 1: Scenarios of system equations and variables [17].

Type 1	$r = m = n$	$\begin{bmatrix} 1 & 0 & 0 \\ 0 & 1 & 0 \\ 0 & 0 & 1 \end{bmatrix}$	$R \rightarrow [I]$
Type 2	$r = m < n$	$\begin{bmatrix} 1 & 0 & 0 & a & c \\ 0 & 1 & 0 & b & d \\ 0 & 0 & 1 & 0 & e \end{bmatrix}$	$R \rightarrow [I\ \ F]$
Type 3	$r = n < m$	$\begin{bmatrix} 1 & 0 \\ 0 & 1 \\ 0 & 0 \\ 0 & 0 \end{bmatrix}$	$R \rightarrow \begin{bmatrix} I \\ F \end{bmatrix}$
Type 4	$r < m, r < n$	$\begin{bmatrix} 1 & 0 & a \\ 0 & 1 & 0 \\ 0 & 0 & 1 \end{bmatrix}$	$R \rightarrow \begin{bmatrix} I & F \\ 0 & 0 \end{bmatrix}$

3.1. Modeling Considerations. In order to analyze the operation of smart devices, we modeled two medium voltage (MV)/LV areas based on real life data. In these regions, the smart solutions have already been operating for years. The modeling also validated the conformity of the implemented SE framework. The topologies are depicted in Figure 4.

For the control models, the on-load tap-changing (OLTC) transformer element of pandapower was used, with the parameters of real devices. The measured data are collected from real measurements of already integrated devices. The examination was conducted with the data for the month of May, 2019. The load behavior is modeled using SLPs. At the time of the integration of these smart devices, the source measurements were known, these were calculated from the reference load flow. Three scenarios were analyzed. In the first one, no smart devices are installed in the networks. At the feed-in point and at the controller locations, a fixed voltage magnitude with known uncertainty is assumed. In the second scenario, smart devices are integrated into the networks, their voltage setpoints are set using predefined measurement series assembled from real life measurement data. In the third scenario, the smart devices' behavior is modeled using load flow simulations, the resulting voltages are then utilized as pseudomeasurements for the state estimation. The topology of the two sites is depicted in Figure 4. On Site A, an OLTC is deployed, while Site B has a series voltage regulator (SVR) around the 1/3 of the circuit length. The loads of both networks were modeled using the regular ZIP model. Each load was represented as a constant impedance, a common assumption for low voltage consumers.

3.2. Framework for Simulations. To analyze the scenarios, a Python-based state estimation framework was devised (the development of the framework is discussed in detail in [26]). The framework uses the pandapower [27] power systems analysis toolbox to create the network model representations and run the analysis.

For the estimation, the WLS algorithm is applied. The estimation is validated using a Newton–Raphson load flow solver (the output of the load flow is the reference for the estimation). Both are implemented and readily available within the pandapower toolbox. The schematic architecture of the pandapower tool and the workflow of the experiments are depicted in Figure 5.

The simulation involves the following steps.

(1) Reading the input files containing measurements, pseudomeasurements, and reference data.
(2) Constructing the digital representation of measurements and pseudomeasurements as internal data structures. These structures enable the data to be readily available for the entire course of the simulation.
(3) Constructing the reference data as a separate data structure.
(4) Reading the physical parameters and topology graph of the network from descriptor files.
(5) Formulating an internal network representation (pandapower format) using the parameters.
(6) Running the state estimation algorithm on the network representation using the input measurements and pseudomeasurements. This step is repeated for a predefined number of steps.
(7) Evaluating a reference load flow as a ground truth for the state estimation using the reference data as an input. The load flow is repeated for the same time steps as the state estimation.
(8) Comparing the output of both the state estimation and the load flow, evaluating the error measure defined in simulation studies. The output of the algorithms is voltage amplitudes and phases of each node for each time step.
(9) Writing the results to the disk as a data table.

Pseudomeasurements are generated in the following manner. SLPs were used to generate pseudomeasurements for each individual household load in the examined networks. SLPs are publicly available in Hungary [28], presenting a realistic consumption profile of Hungarian LV consumers. The DSO has applied these curves for network planning traditionally and also to predict electricity consumption.

The applied dataset contains consumer curves for multiple load types, of which we used the simple LV household consumer curve and the PV generation curve for generation. The profiles include the consumption rates for the whole of 2022 in a 15-minute resolution. To obtain the actual power values, the selected curve was scaled by each of the modeled consumers' average annual consumption, and the resulting time series were trimmed to the simulation period (a 30-day period in the month of May). Reactive power consumption was directly calculated from the active power values using a power factor of 0.98, as there were no data from the customer's reactive power consumption. The goal was to show the effects of the smart assets, and for the sake of clarity, the loads are kept in an ordinary state. The research could be expanded with further simulations, e.g., stochastic load profiles and enhanced level of PV generation, but those scenarios should be carried out as a sensitivity analysis. In this study, we only focused on the quantitative examination of the smart asset effects, which were integrated into this WLS-based DSSE framework as a new data source.

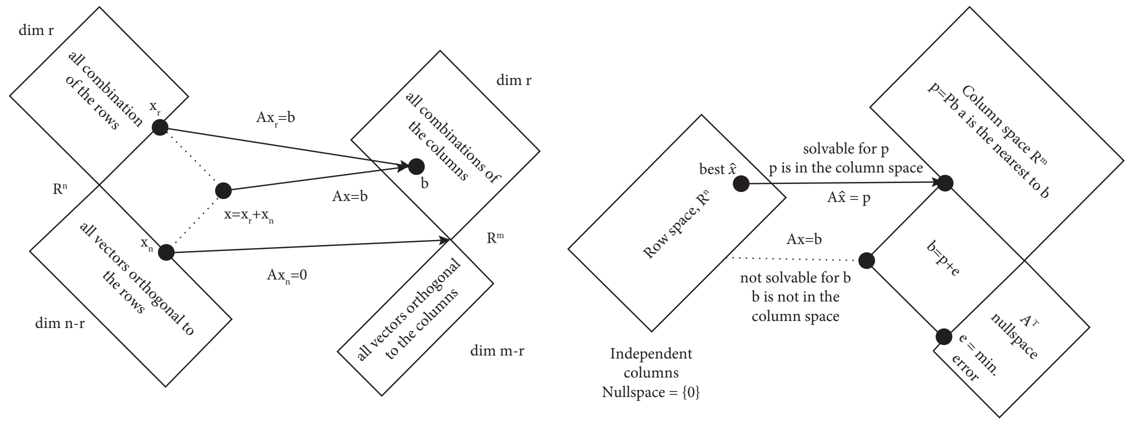

(a) (b)

Figure 2: Geometric meaning of the two types of equations [17].

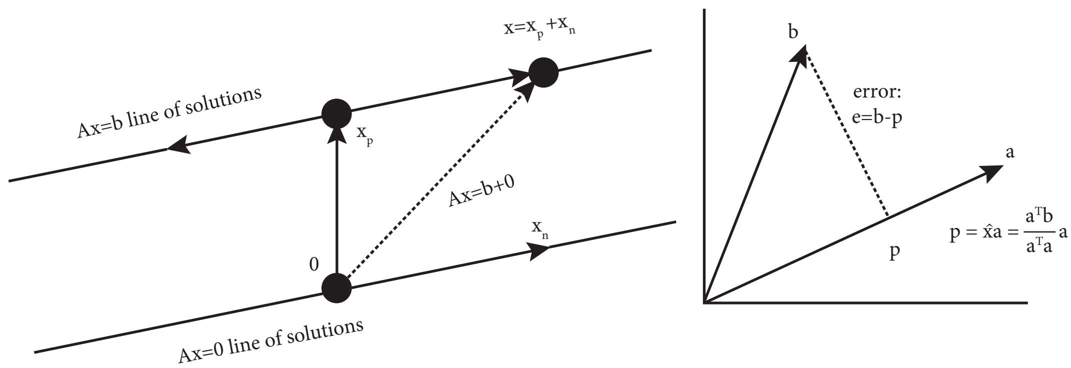

(a) (b)

Figure 3: Many solutions with free variables vs. solution with projection [17].

3.3. Load Profiles and Voltage Measurements. The resulting pseudomeasurement files contain active and reactive power consumptions for each node of the simulated networks. The data is in a quarter-hour resolution. Behind each node, multiple loads and generators can reside in the network, the loading and feed-in of these elements are aggregated prior to the simulation and represented as a single data-series for each customer connection point.

State estimation determines which network state has the highest likelihood, using the reliability of measurements as a starting point. This means, measurements with a lower level of uncertainty are regarded as more reliable, and thus are taken into account with a higher weight. For an informative scenario modeling, it is indispensable to set the values of uncertainty, realistically. For each type of input data, the following measurement uncertainties were used.

3.3.1. P and Q Profiles. The SLPs used to generate individual household loads are representative profiles and are typical on average by the respective group to be modeled. The quality of pseudomeasurements based on SLPs are, thus, largely affected by the size of the group on which the assumption is made. The uncertainty of these profiles may be much larger than the measurements, especially for the case presented, where the time stamps of the voltage and power measurements are not strictly aligned, and there is a small, nonrepresentative set of loads and generators in the network. We assume a large uncertainty (1 kW) for the loads for the state estimation, which on average yields a 200% error margin for the power measurements (average consumption is 0.5 kW).

3.3.2. External Grid Voltage and Voltage at the Controller for the Noncontrolled Scenario. The uncertainty of the external grid and noncontrolled scenario voltage measurements are based on the error of standard voltage measurement devices, which is 3%. For the state estimation, the uncertainty of the measurements are taken into account with a standard deviation of 1%, assuming a Gaussian error distribution. In the load flow process, external grid measurements are considered as error-free and are used to constrain the solution of the power flow equations. In both regions, measurements from the external grid were available at a resolution of 10 minutes, which were then resampled to a resolution of 15 minutes. Figure 6 shows the time series data.

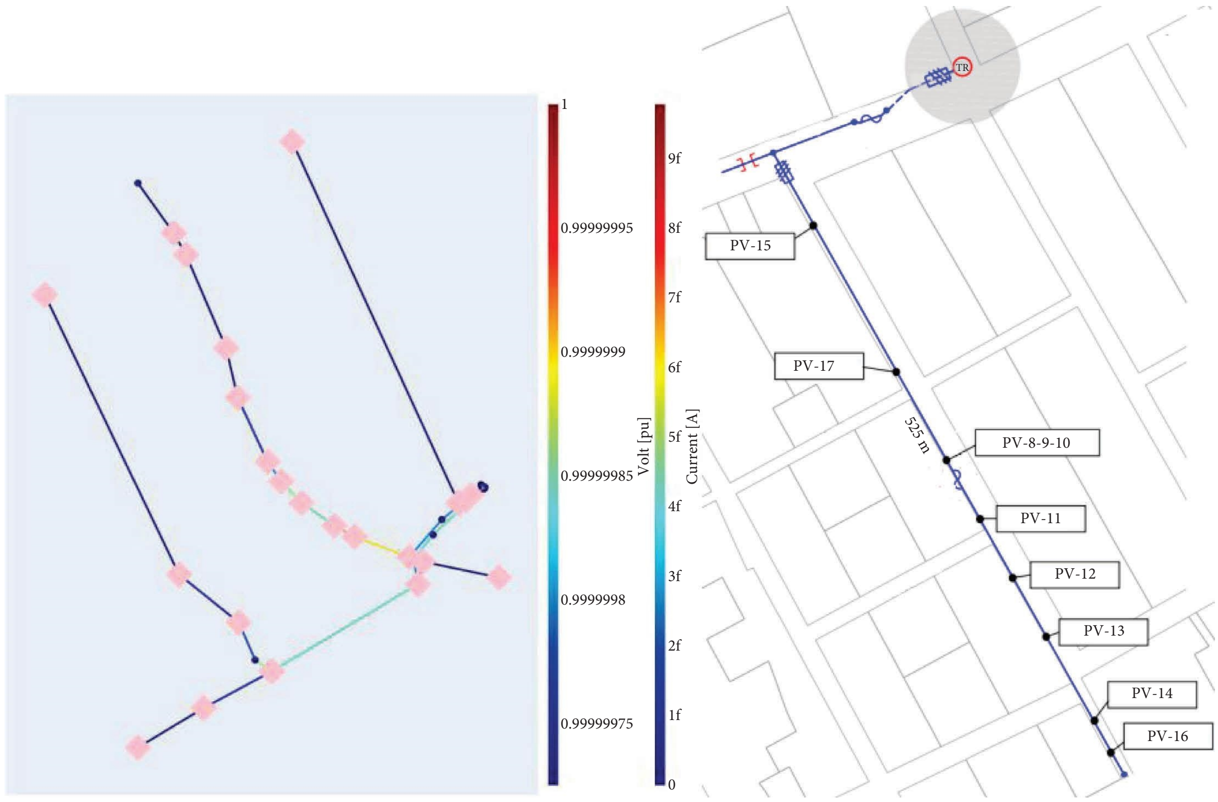

(a) (b)

Figure 4: Topology of the examined sites: site A (a) and site B (b).

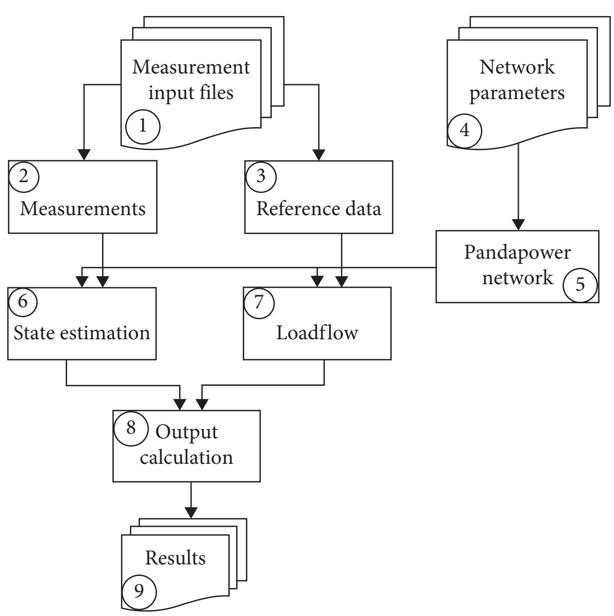

Figure 5: The workflow of the estimation framework. Input files are read and processed, then fed to the estimation and load flow algorithms. The SE results are then validated and written to file.

3.3.3. Controller Voltage. The uncertainty of the voltage measurements at the controllers is based on the controller tolerance around the setpoint voltage, which is 1.5%. The uncertainty for the state estimation is set to 0.5%, assuming a Gaussian error standard deviation. The rationale behind the assumption of an uncertainty of 1.5% for the voltage measurement at the SVR control device is based on the calibration characteristics of the SVR device, as we assume

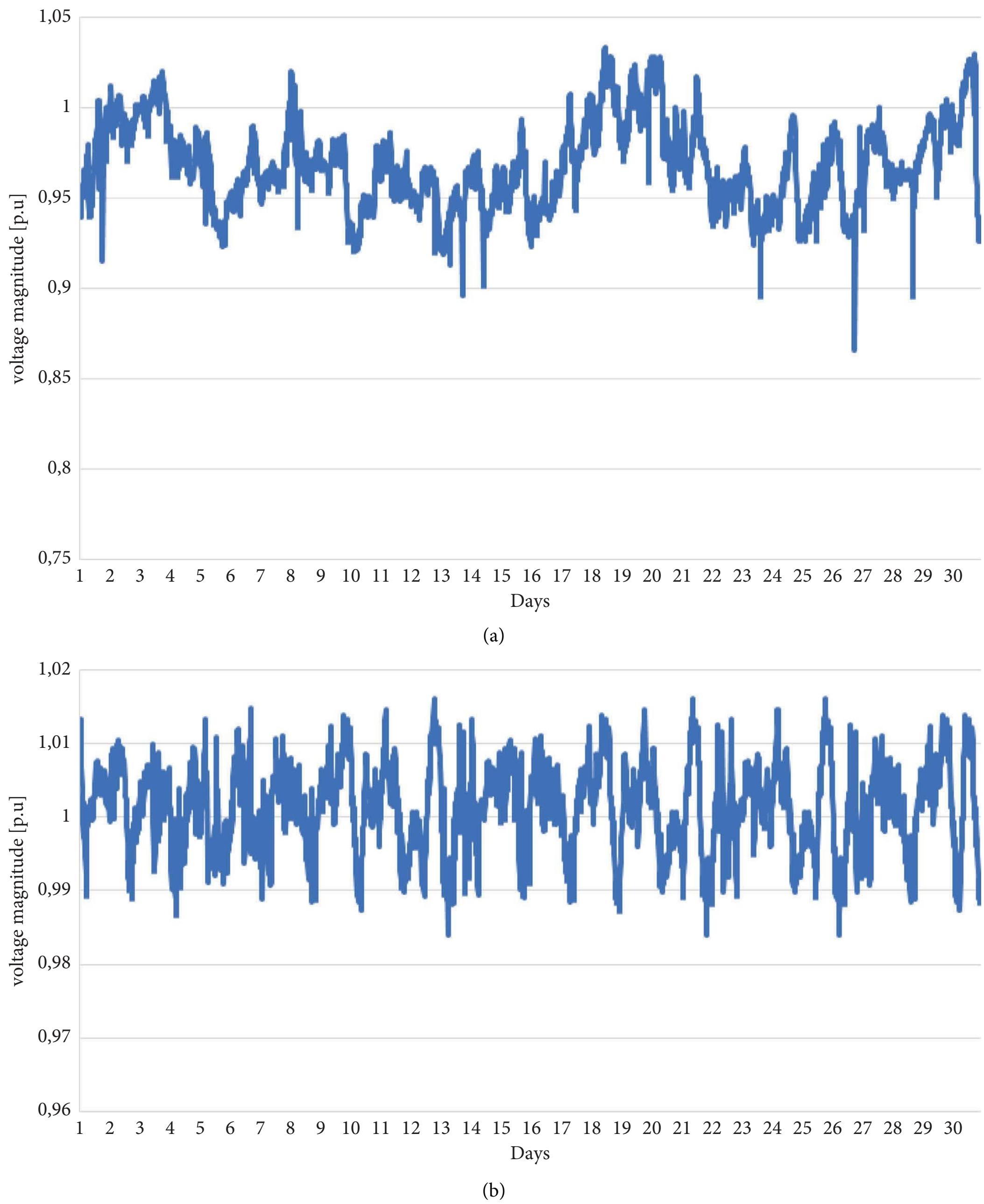

Figure 6: External grid measurements: site A (a) and site B (b).

that the regulator can control the voltage with this error margin around the setpoint voltage (1 p.u.). For the load flow process, the controller voltage is considered error-free.

In the second scenario, synthetic measurements called "pseudomeasurements" were utilized. These were generated through the use of a Python loop that implemented the control logic of an actual OLTC transformer. Since the data set used was obtained from the secondary side of the previous transformer, the resulting output was similar to real data (Figure 7).

Compared to the SLP pseudomeasurements, these controller-based pseudomeasurements, as new kinds of pseudomeasurement sources result in lower standard deviation in LV DSSE, similarly to real measurements, thus they enable a more precise state estimation. SLPs are commonly used in studies, while the controller-based data presented for example in Figure 7 are introduced in this paper. This is an extension of the currently achievable DSSE, as DSOs lack the availability of online data and pseudomeasurements as well. We focused on 2 devices which are getting more common on the LV level, but the technique can be extended on any controller or smart asset. Also, using the historical data as pseudomeasurement does not require any investments to create a measurement integration. To compare the values of the latter, the paper analyses both solutions: pseudomeasurement generation from historical data and measurement integration. At Site B, no on-field

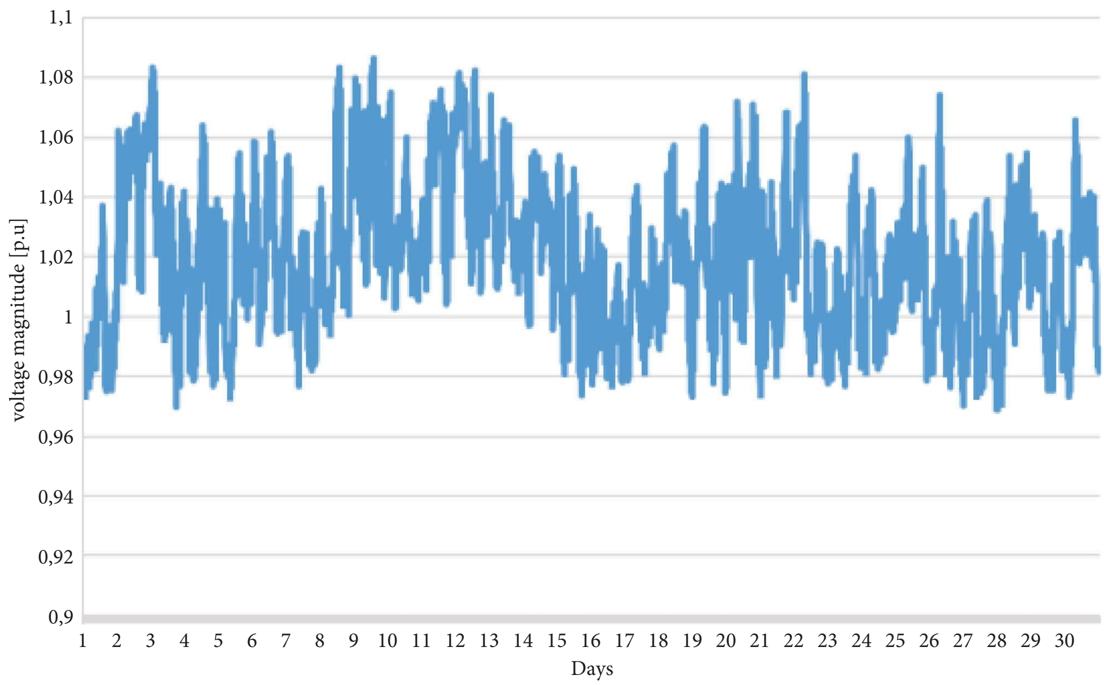

(a)

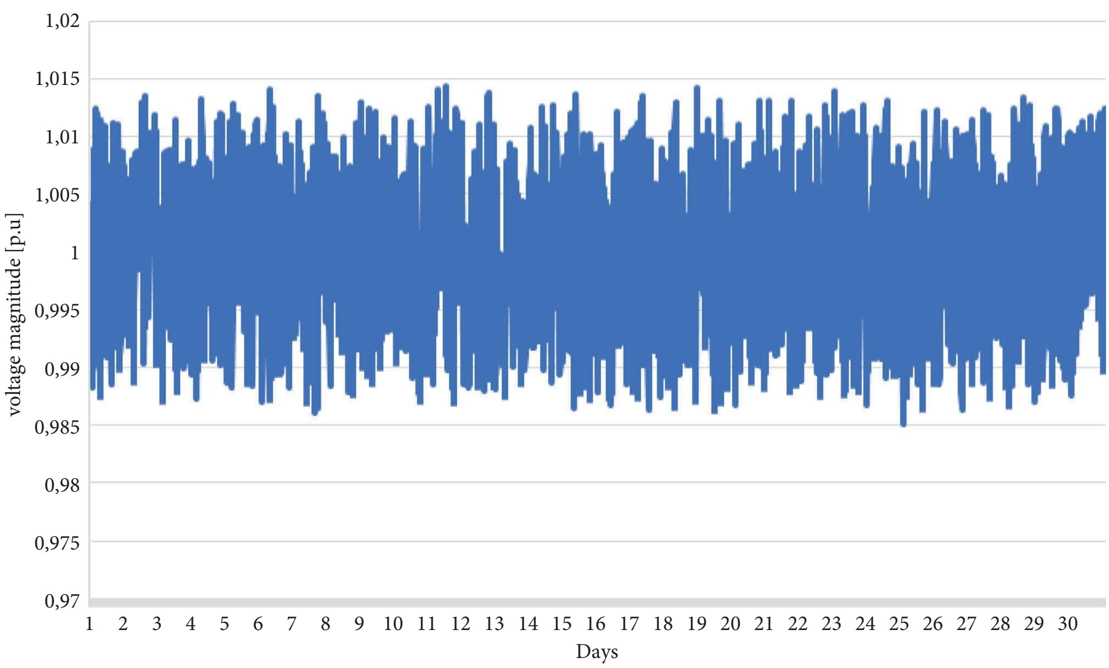

(b)

Figure 7: OLTC measurement (a) and pseudomeasurement for control state (b).

measurement is necessary to create the pseudovalues. The secondary side of the SVR control device can be assumed to have a voltage magnitude of 1 p.u., with an uncertainty of less than 0.5% (0.005 p.u.) as specified above.

3.4. Smart Assets in the DSSE Process. DSOs are currently embracing different smart grid solutions, which our research group reviewed in a previous paper thoroughly [29]. At the high voltage substation level, OLTC transformers are extensively applied; meanwhile, MV/LV transformers usually lack this device. Controlled voltage can be ensured by power electronic converter-based SVRs at a certain node, as a result of which the volatility of the voltage is considerably decreased along the radial line. In LV pilot projects, energy storage systems, i.e., battery technologies together with the distributed generator's inverter control are capable of controlling state variables at a given grid point. Loads in direct load control systems may be predicted more accurately, and thus may be regarded as reliable pseudomeasurements. This paper analyses two assets from the viewpoint of DSSE integration, the OLTC, and the SVR, respectively.

MV/LV transformers are generally characterized by fixed tap positions. These are altered only if the equipment is de-energized. In the course of the commission, the electricians position the taps following the guidelines. However, if the MV loading conditions result in the MV voltage fluctuating higher than usual, or the LV customers cause large voltage changes, an OLTC might be a viable technical solution. Regarding the LV circuits, OLTC is more efficient if the voltage profile of the circuits supplied by the transformer is similar, because it controls the whole secondary substation area. As for higher seasonal variance, which might occur in a holiday resort area, loads may significantly differ in various times of the year. The control dynamics can be safely neglected in the static condition DSSE, as the duration of the transient caused by tap-changing is significantly shorter than the time step of the DSSE, which uses one-minute averages for the simulation. Measurements from the LV terminal are also provided by the OLTC transformer. Figure 8 shows the operation principle of the OLTC; there is a regulation bandwidth around the nominal terminal voltage. If the voltage stays within the regulation bandwidth, no control action happens. When the LV terminal voltage goes outside the regulation bandwidth due to changing load conditions, the OLTC controller (after a preset delay time) switches the tap to bring the voltage back into the regulation bandwidth.

As the penetration of renewable energy sources increased, power electronic converters as voltage regulators have also become more common. Such devices, which may be connected either serially or in parallel, accurately control node voltages in a flexible manner. The control dynamics may be neglected (even with the commercially available devices with discrete steps). The connection of an inverter-based SVR is depicted in Figure 9. The voltage levels of a system with and without an SVR from a Hungarian pilot project [29] are shown in Figure 10. Basically, the main task of an SVR is to divide the circuit into two parts. Starting from the LV busbar, which is generally characterized by a slightly fluctuating voltage, to the SVR, the connected loads modify the voltage profile depending on their current operation points. The SVR should be mounted on the pole to the grid at the point where the voltage profile is sure to remain within the limits without any control, where it provides controlled voltage for the rest of the network. The SVR provides voltage control downstream from the mounting point. When the SVR operates, this point behaves similar to a feeding point with high short-circuit power. The controller maintains a preset voltage at the regulated point within a strict limit, practically constant.

This application separates the electric circuit into two distinct parts, which reduces the volatility of the voltage profile, and at the same time implicitly provides voltage magnitude pseudomeasurements of constant value at the controlled point due to the fixed setpoint. In this context, SVR could become an important data source in the LV DSSE algorithm. Table 2 summarizes the data sources used in the simulations.

Figure 10 shows the voltage at the two sides of the SVR-uncontrolled point (Figure 10(a)) and SVR controlled point (Figure 10(b)) [29].

4. Simulation Studies

The goals with the implementation of state estimation augmented with smart solutions are as follows:

(i) Analysis of the range of low voltage smart devices and their integration into state estimation

(ii) The integration of low voltage SVR and OLTC models into

  (1) Load flow calculations
  (2) State estimation with pseudomeasurement data
  (3) State estimation with real measurement data

(iii) Case study for a period of 1 month

  (4) Without control devices
  (5) Modeling control devices with pseudomeasurements (in the absence of real measurements)
  (6) Modeling control devices with real measurements (measurements with known uncertainty)

The simulation results were evaluated by using an error metric defined as the root mean square difference between the reference load flow and the results obtained from the suggested DSSE method. In this system, the reference load flow serves as an appropriate benchmark to establish a virtual scenario, from which the proposed method results can be compared and the effects of integrating smart assets on the power system can be observed in terms of both space and time. Additionally, this approach can be further validated if online measurements are available on the sites, as the installation of such devices is ongoing. Therefore, the results presented in this paper will be validated in practice in the future.

The paper evaluates the state estimation performance by observing the voltage profile over 2880 time steps and calculating the mean difference throughout this simulation period. This method provides a more comprehensive understanding of the various operation states and conditions of the networks and the accuracy of the state estimation algorithm under these conditions compared to an ad hoc Monte Carlo test, which may only analyze individual time steps but fails to systematically evaluate the accuracy over the entire simulation period.

4.1. Simulation Studies: Site A. In the first case, the base state of the network was calculated, without the OLTC. For each scenario, the external grid voltage profile is used as a pseudomeasurement. In each scenario, we used box plots to show the variation of the voltage on a given node, in per unit values. This method helps to visualize the behavior of the values in only 1 diagram. In each case, there are 3 output

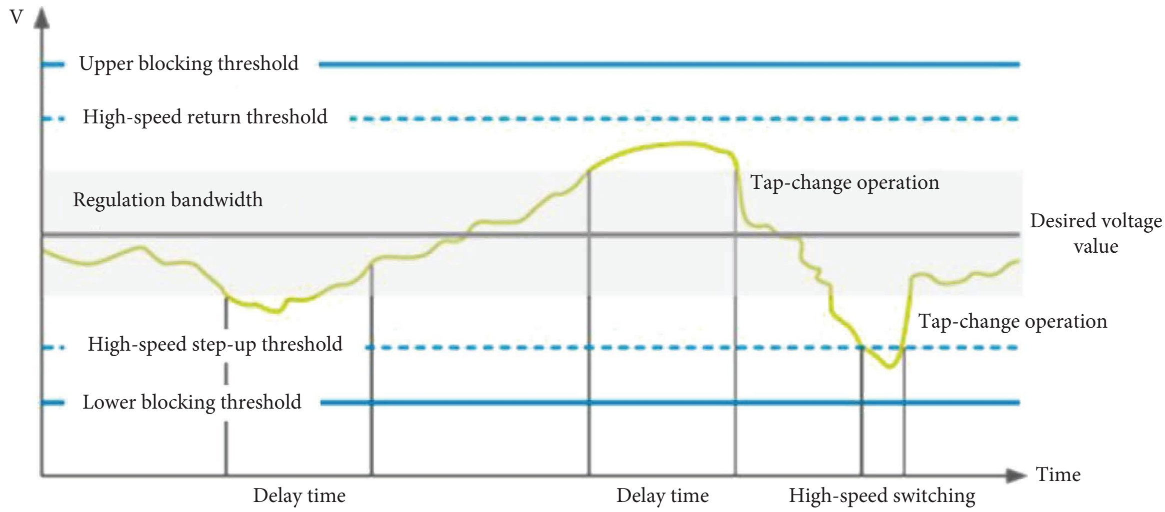

FIGURE 8: Example operation of the OLTC transformer [30].

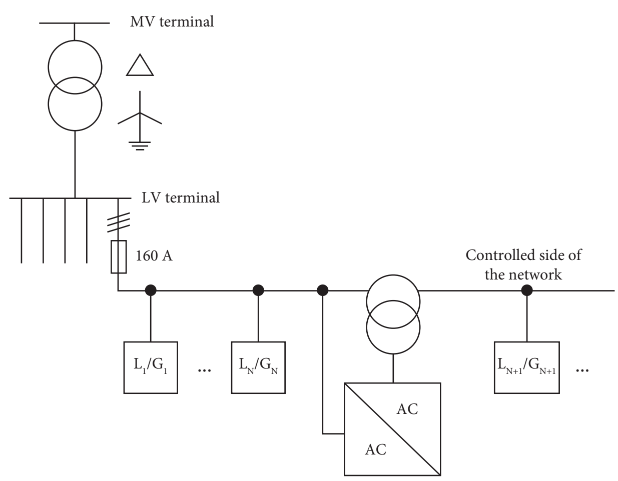

FIGURE 9: SVR connection scheme [29].

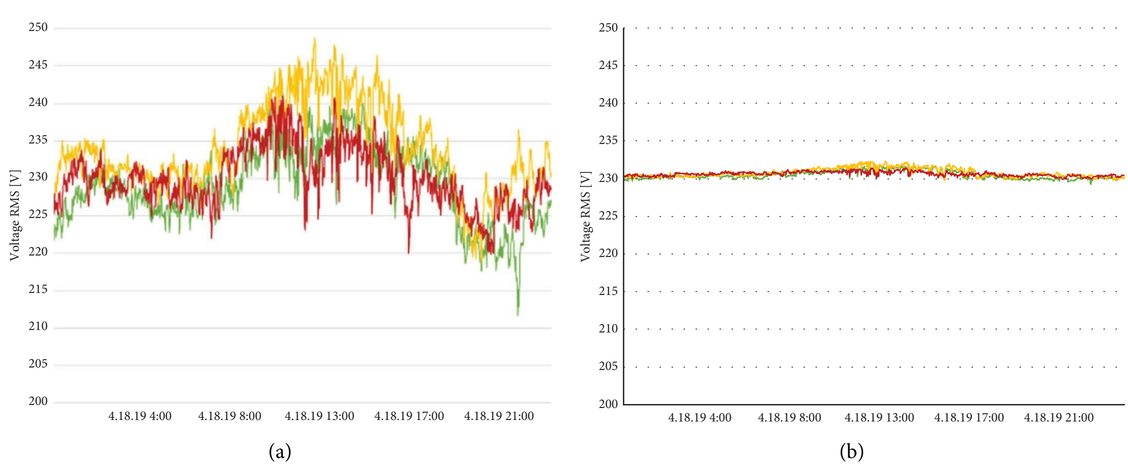

FIGURE 10: Voltage at a given node before the SVR application and after the SVR application.

diagrams. The first one is the voltage magnitude result of DSSE, the second is the reference load flow result, and the third is the difference between the two calculations (error).

In the case of SVR, it is assumed that if the device is deployed, an LV terminal measurement is also present. Figure 11 depicts the base case results for Site A. In each

Table 2: Data sources of the simulations.

Datasets		Site A OLTC			Site B SVR	
Measured node	Uncontrolled scenario	Pseudomeasurement scenario	Controlled scenario with measurements	Uncontrolled scenario	Pseudomeasurement scenario	Controlled scenario with measurements
OLTC/IVR control point, LV terminal	Ordinary transformer measurements from LV terminal	Generated pseudo measurement with the logic of a real OLTC	Reference load flow "measurements"	Ordinary transformer measurements from LV terminal	Constant value of 1 p.u (with uncertainty)	Reference load flow "measurements"
Load	SLP	SLP	SLP	SLP	SLP	SLP
MV voltage	External grid measurements	External grid measurements	External grid measurements	External grid measurements	External grid measurements	External grid measurements

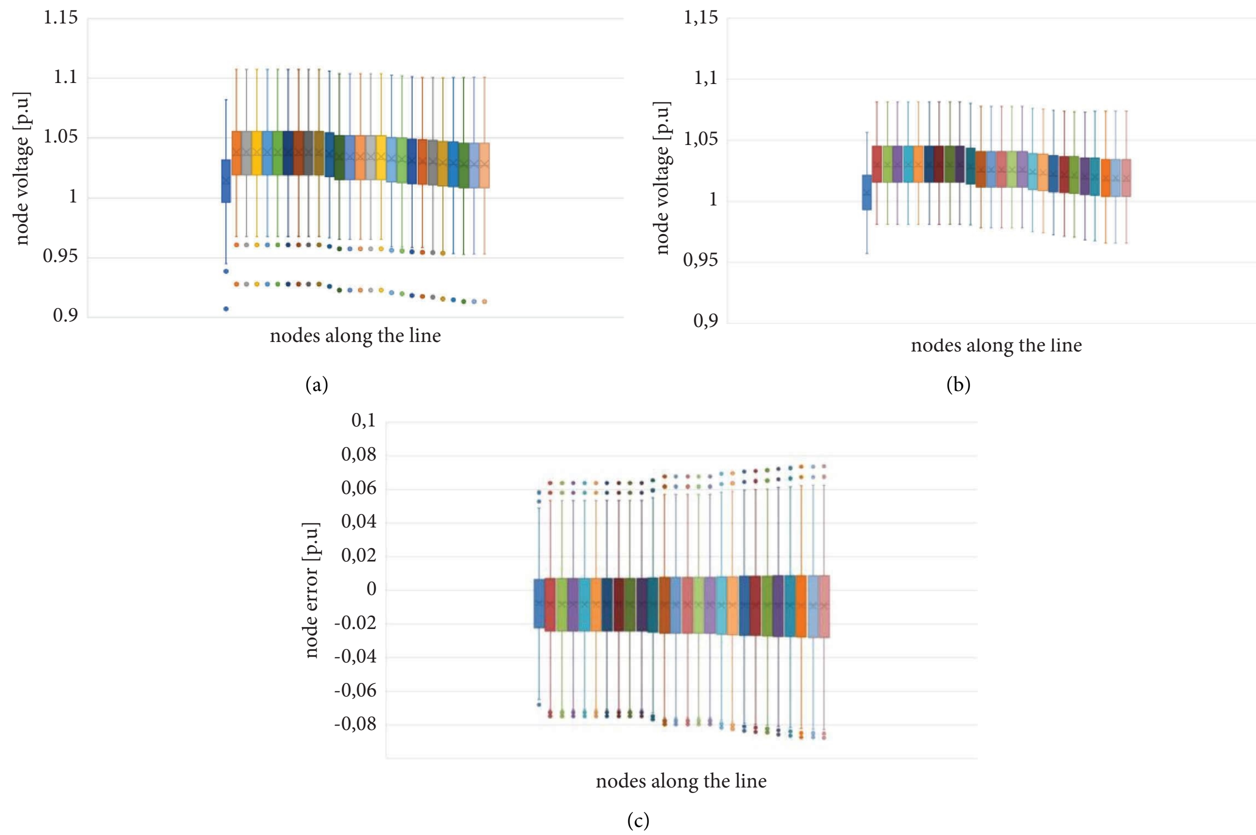

Figure 11: Site A: base case results. State estimation (a), load flow (b), and error (c).

simulation, the blue frame depicts the state estimation voltage magnitude results (green is for the load flow, while the red frame shows the error).

In the case of Site A, one circuit was considered from the transformer to the endpoint to have clear results along the line. The voltage does not fluctuate greatly on the grid, which is the result of simplified load modeling. However, it can be considered a realistic scenario and appropriate for the smart asset analysis.

The blue rectangle on the left is the MV external grid. The large difference between the first two nodes is due to the settings of the transformer. For the first scenario, measurements from the transformer sides were used. In the results from the first scenario of Site A, one can see a jump in the voltage magnitude. This jump originates from the tap settings of the transformer. The typical setting for MV/LV transformer taps is to provide the mean value of 1.03 p.u on the LV terminal. With that in mind, we had real measured data from the region. The primary side measurements were 22 kV (or around 1 p.u), but the secondary side, keeping in mind the previously mentioned reason, were above the per unit. In other simulations, it does not occur due to the fact that smart assets are applied, not the conventional development guidelines.

The voltage profile is smooth along the circuit, the voltage and error curves are similar to that of other LV DSSE implementations. The error slightly increases from the transformer's LV terminal to the endpoint due to the uncertainty of the connecting parallel elements. The error is in the range of ± 0.02 per unit most of the time.

The case utilizing pseudomeasurements is shown in Figure 12 (Scenario 2). The OLTC's effect on the voltage magnitudes can be observed. The voltage variation is decreased compared to Scenario 1, and this effect propagates along the line. The error of the simulation is overall reduced, and this is mainly due to the smaller fluctuations in the input values, which leads to a significant improvement in DSSE accuracy.

The case where the OLTC measurements are directly integrated into the DSSE is shown in Figure 13 (Scenario 3). Here, the voltage profile does not change drastically from the pseudomeasurement case (OLTC was applied and had effect in those cases, which is a difference compared to the base case), but the error is reduced by orders of magnitude due to the improved accuracy of the used measurement. Meanwhile, the spatiality of error is also changed. There is a greater relative increase along the line from the accurate measurement to the more uncertain endpoint. However, any error here is much smaller than in the previous scenarios.

4.2. Simulation Studies: Site B. In the first case, the base case state of the area (without the SVR) was calculated similarly to the OLTC network. The external grid voltage profiles were used as input for this network as well. Here, the difference between the MV and LV terminal voltage equals the

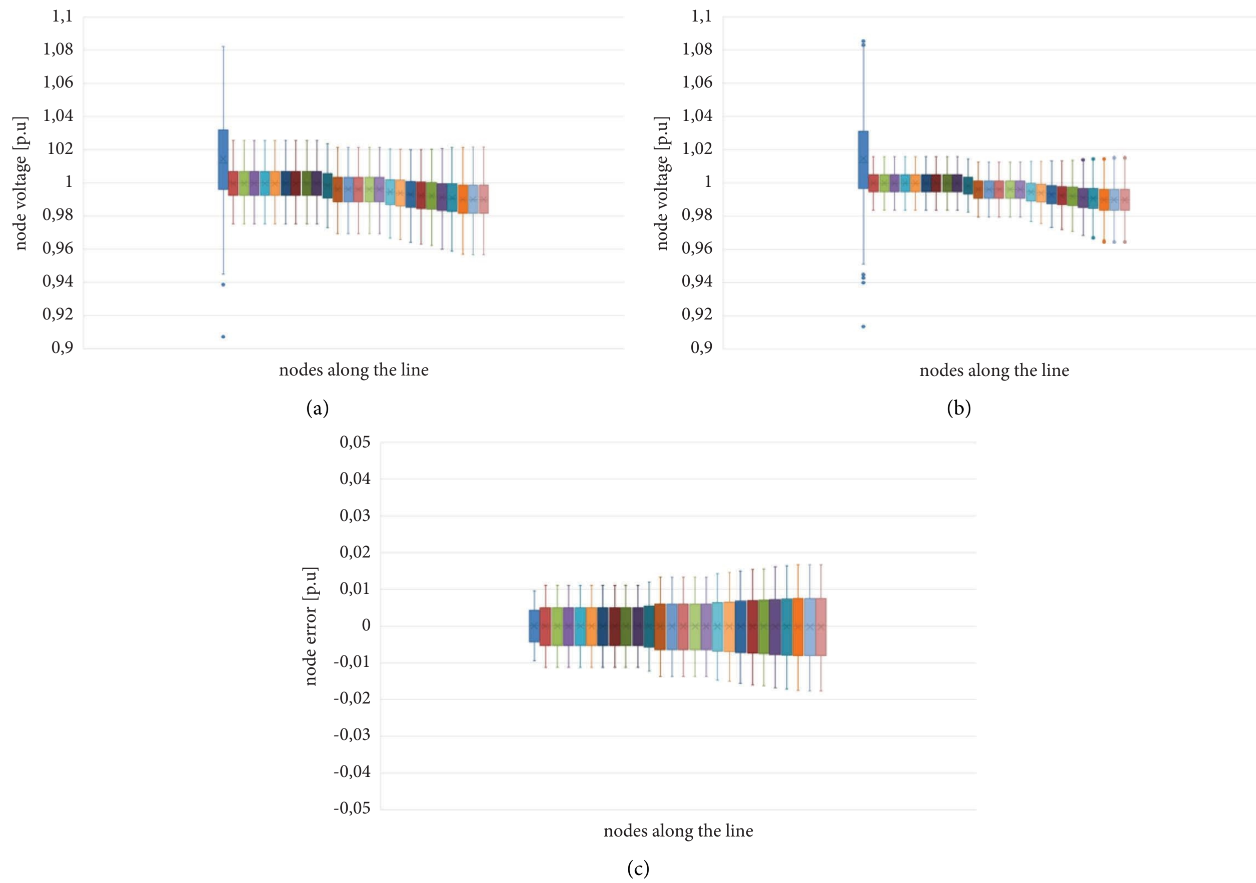

Figure 12: Site A: pseudocase results. State estimation (a), load flow (b), and error (c).

transformer drop. After the feed-in point, the voltage magnitudes along the line are depicted using box plots. The circuit shows the expected behavior, as the voltage variation and the error increases from the LV terminal to the endpoint (Figure 14).

The pseudomeasurement scenario (Scenario 2) is depicted in Figure 15. Here, we can see a large error reduction, as well as the expected change in the voltage profile due to the SVR. The device is connected between nodes 13 (light blue) and 14 (light red), and the setpoint of the controlled node is 1 per unit. The voltage variation shows the expected pattern, it increases from the LV terminal until the last uncontrolled point, then the SVR control greatly reduces it, and until the endpoint, the monotonous increase appears again. The error decreases by one order of magnitude in comparison to the first scenario, as seen in Figures 14 and 15. Despite the presence of the SVR, the error profile remains unchanged, which is likely due to the pseudomeasurements not accurately reflecting the operational conditions at the regulated point.

The measurement-integrated case (Scenario 3) is shown in Figure 16. The error is further reduced. However, the voltage variation does not differ from the previous (pseudomeasurement) scenario. Another interesting remark is the error's spatiality. The proximity of the SVR lowers the error, as well as the LV terminal measurement, and from the measured points to the end of the line, the error increases again. The decreased error profile observed is believed to be a result of the regulated point voltage being derived from the load flow simulation. This measurement provides a closer alignment with the benchmark conditions compared to the pseudomeasurements utilized in Scenario 2, leading to a reduction in the error at the regulated point and at its vicinity.

As a result, it can be concluded that even the integration of the control principles via low-uncertainty pseudomeasurements have a good effect on the estimation accuracy. The main conclusion is that the measurement-integrated scenario has proven to be the most accurate and useful for modeling and monitoring LV networks with smart assets.

Another conclusion is that the error results (the red blocks) in Figures 11, 13, and 14 show that the state estimation results are strongly biased, with the error tending to be negative. This is surprising, as the weighted least squares (WLS) method, which is used in the work, is known to be an unbiased estimator under Gaussian noise assumptions.

It appears that the bias in the error results is due to the definition of error used in the paper, which is the difference between the load flow and state estimation results, rather than the estimation error, which would be the difference

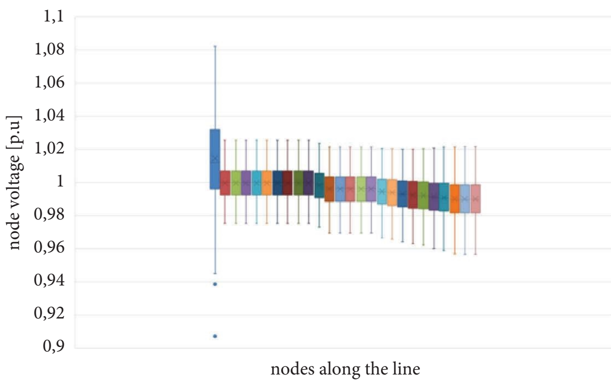

(a)

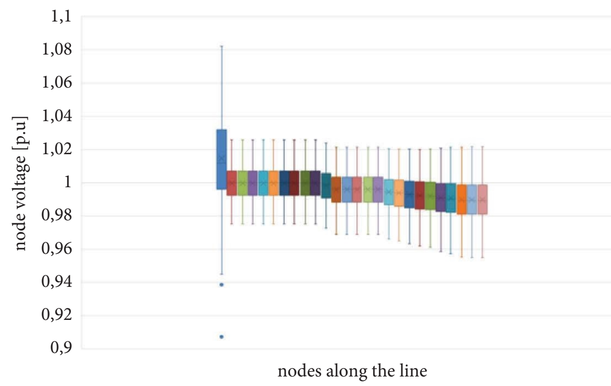

(b)

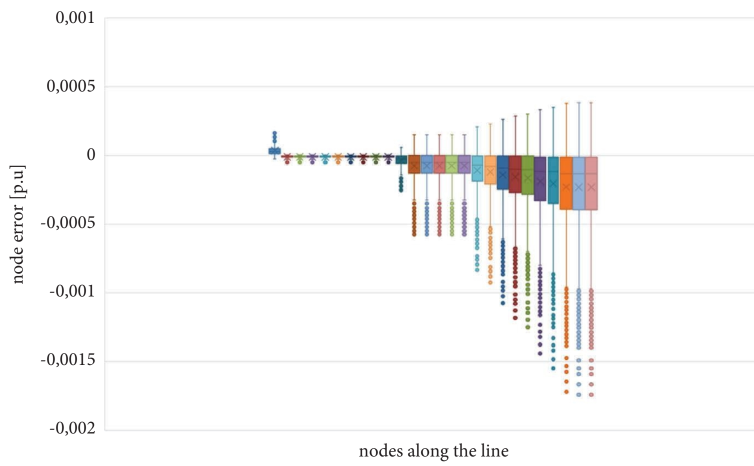

(c)

Figure 13: Site A: measurement-integrated case results. State estimation (a), load flow (b), and error (c).

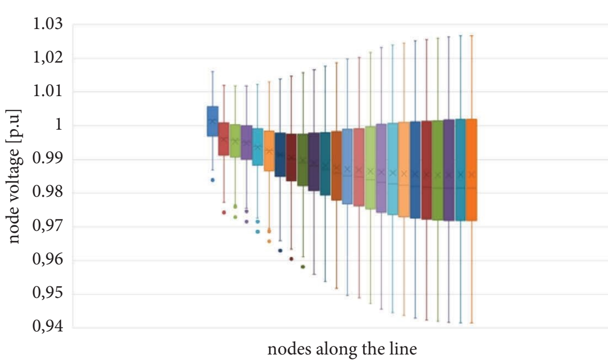

(a)

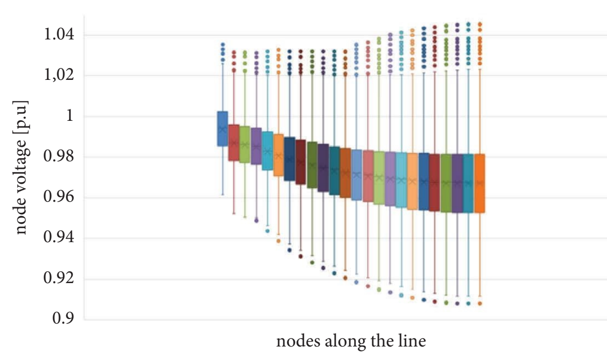

(b)

Figure 14: Continued.

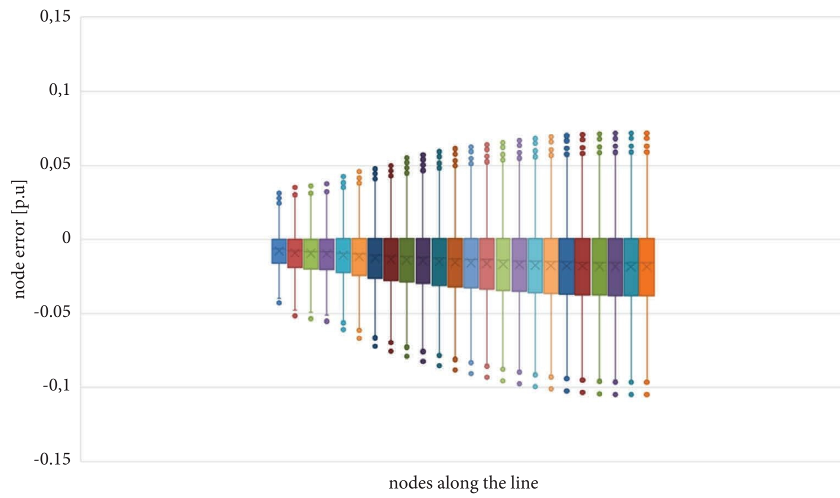

(c)

Figure 14: Site B: base case results. State estimation (a), load flow (b), and error (c).

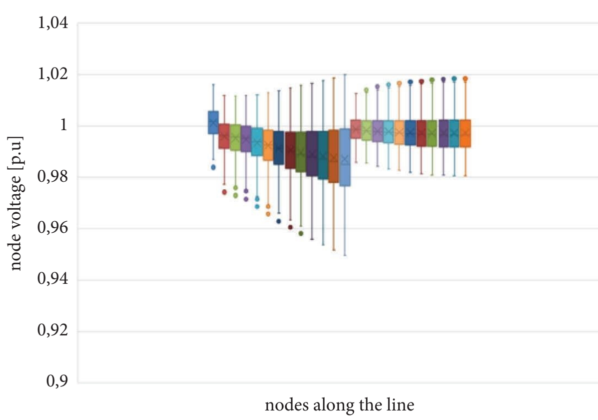

(a)

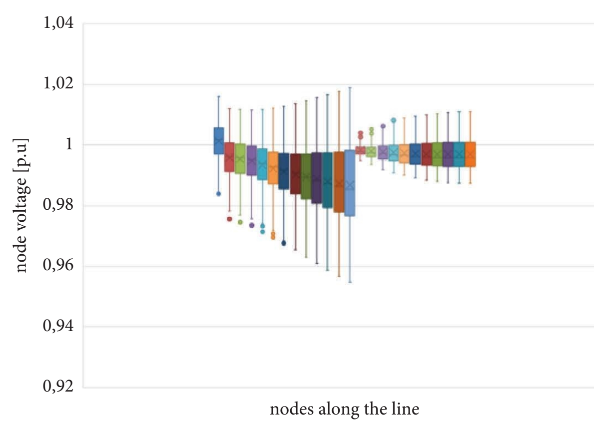

(b)

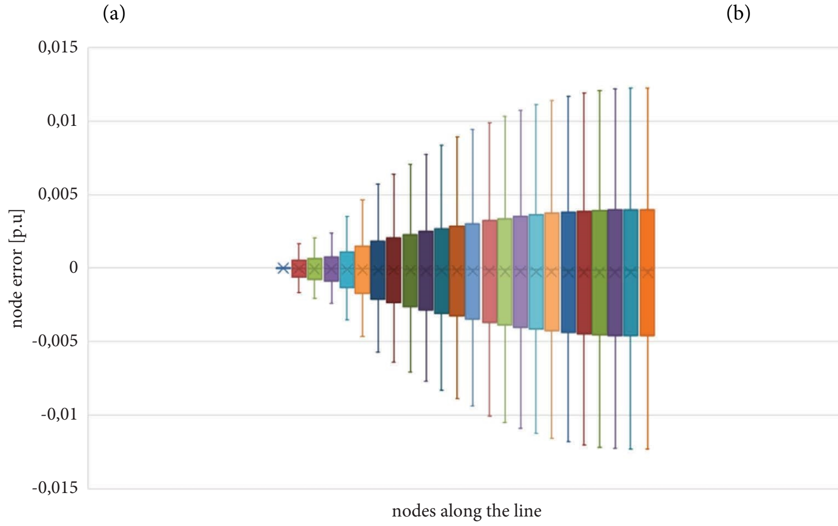

(c)

Figure 15: Site B: pseudocase results. State estimation (a), load flow (b), and error (c).

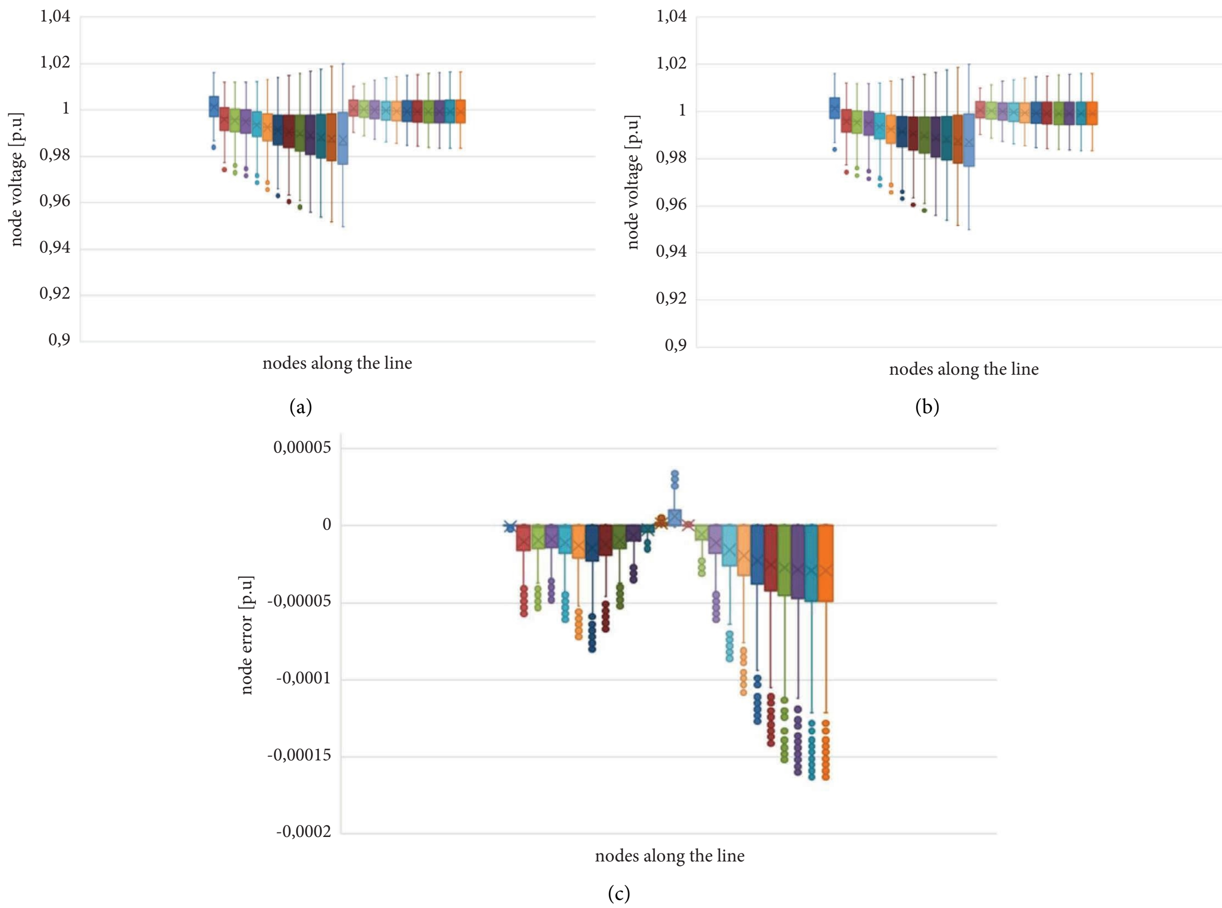

Figure 16: Site B: measurement-integrated case results. State estimation (a), load flow (b), and error (c).

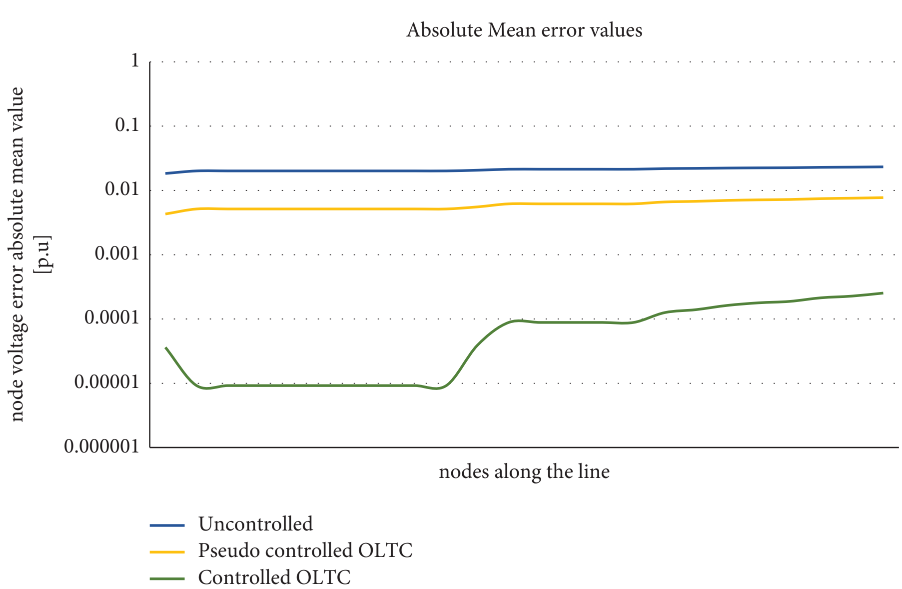

Figure 17: Site A errors in different scenarios.

between the true state of the system and the estimated state. This difference in definition may explain why the error results are showing a negative bias, as it appears to be a positive difference in the load flow results compared to the true state of the system. This positive difference is likely due to inaccuracies in the assumed power values at feed-in points, which is causing the load flow results to be higher than the true state of the system.

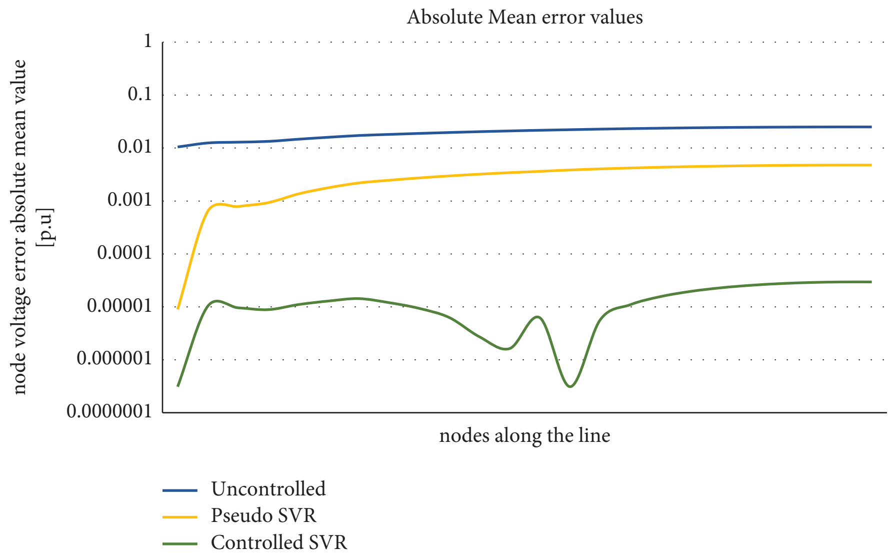

Figure 18: Site B errors in different scenarios.

5. Conclusions

This paper examined the concept of smart asset, namely, OLTC and SVR, integration into the DSSE process. First, it was outlined that LV DSSE lacks the reliable metering data, and that due to the distributed generation, electrification, and active customers, distribution system operators have already deployed smart assets at many sites. These devices locally control voltage; furthermore, they can transmit measured data to the system operators, which can be channeled into a DSSE framework to increase network observability. Our research group developed a DSSE analysis framework and modeled two real LV network sites to analyze the operation of such assets and their effect on state estimation accuracy. The sites have the devices already installed; therefore, the input data for the simulation is considered realistic. The goal was to show that the devices reduce the estimation errors. Currently, there is no real-time transmission of the measured data yet; therefore, load flow simulations were created as a reference.

The results show that using the SVR and OLTC setpoints as pseudomeasurement data reduces the error by an order of magnitude, while using them as online measurements further reduces the error by another order of magnitude. Figures 17 and 18 show the error comparison on the sites. Regarding Site A, the customer connections caused a change in the error (there are no loads at the beginning of the line), while at Site B, the monotonicity changes due to the SVR. The error distribution along the line also proved that if the SVR is integrated, it reduces the error greatly in the proximity (Figure 16). However, with the current SVR tolerance settings, the error function spatiality finding was not extendable to the pseudomeasurement case, as the voltage bound of the controller is in the range of the error of the controller voltage pseudomeasurement of the DSSE, resulting in a somewhat larger error at the control point compared the integrated case. The OLTC scenario showed the expected results, as the error was reduced, but there was no change in its spatial distribution. Both smart assets showed good results in terms of voltage control before; this paper described the possibilities to use the voltage control devices as a data source for DSSE, either as a control, function driven, highly reliable pseudomeasurement, or as an integrated real measurement.

In the next steps, meters will be installed on the sites, which will create an opportunity to compare the DSSE results to actual online measurements. With this extension, these results are expected to create an expansion in the WLS DSSE framework algorithm, to integrate smart assets as data sources.

Figures 17 and 18 illustrate the advantages of our methodology compared to the base case DSSE. The pseudomeasurements used in the case depicted with yellow are easily accessible with the manipulation of real measurements from the site (therefore, can applied without integrating communication systems for measurements), which later can be reused in the DSSE. It is also noticeable that the use of these data mitigated the value of error in both cases, especially in case of the SVR, where between the base case DSSE and the pseudodata DSSE, a reduction of an order of magnitude is present. This means that the use of innovative tools contributes greatly to accuracy and the data considered in this method are accessible for operators who use such equipment.

Nomenclature

DSSE: Distribution system state estimation
LV: Low voltage
MV: Medium voltage
OLTC: On-load tap-changing
PMU: Phasor measurement unit
PV: Photovoltaic
SCADA: Supervisory control and data acquisition
SLP: Synthetic load profile
SVR: Serial voltage regulator

WLS: Weighted least square
ZIP: Constant impedance, constant current, and constant power.

Data Availability

The data used to support the findings of this study are available from the corresponding author upon request.

Conflicts of Interest

The authors declare that they have no conflicts of interest.

Acknowledgments

This research was supported by the Hungarian Academy of Sciences and E.ON Hungary through the "Célzott Lendület" Program application of the MTA-BME FASTER Research Group and with the professional support of the Doctoral Student Scholarship Program of the Cooperative Doctoral Program of the Ministry for Innovation and Technology from the source of the National Research, Development and Innovation Fund. The authors acknowledge the open access funding enabled and organized by Electronic Information Service National Programme.

References

[1] R. H. A. Zubo, G. Mokryani, H.-S. Rajamani, J. Aghaei, T. Niknam, and P. Pillai, "Operation and planning of distribution networks with integration of renewable distributed generators considering uncertainties: a review," *Renewable and Sustainable Energy Reviews*, vol. 72, pp. 1177–1198, 2017.

[2] N. Mahmud and A. Zahedi, "Review of control strategies for voltage regulation of the smart distribution network with high penetration of renewable distributed generation," *Renewable and Sustainable Energy Reviews*, vol. 64, pp. 582–595, 2016.

[3] T. Xu and P. C. Taylor, "Voltage control techniques for electrical distribution networks including distributed generation," *IFAC Proceedings Volumes*, vol. 41, no. 2, pp. 11967–11971, 2008.

[4] F. Ahmad, A. Rasool, E. Ozsoy, R. Sekar, A. Sabanovic, and M. Elitas, "Distribution system state estimation-A step towards smart grid," *Renewable and Sustainable Energy Reviews*, vol. 81, no. 2, pp. 2659–2671, 2018.

[5] A. Primadanto and C. N. Lu, "A review on distribution system state estimation," *IEEE Transactions on Power Systems*, vol. 32, no. 5, pp. 3875–3883, 2016.

[6] A. Abdolahi and N. T. Kalantari, "State estimation of asymmetrical distribution networks by μ-PMU allocation: a novel stochastic two-stage programming," *Electric Power Systems Research*, vol. 213, Article ID 108738, 2022.

[7] Z. Cao, Y. Wang, C.-C. Chu, and R. Gadh, "Robust pseudo-measurement modeling for three-phase distribution systems state estimation," *Electric Power Systems Research*, vol. 180, Article ID 106138, 2020.

[8] J. H. Teng, "Using voltage measurements to improve the results of branch-current based state estimators for distribution systems," *IEE Proceedings- Generation, Transmission and Distribution*, vol. 149, no. 6, p. 667, 2002.

[9] M. S. I. Neto and E. N. Asada, "Considerations on three-phase modelling for branch-current state estimation," *Electric Power Systems Research*, vol. 213, Article ID 108532, 2022.

[10] J. Huang, X. Zhou, and B. Cui, "Online distribution system state estimation via stochastic gradient algorithm," *Electric Power Systems Research*, vol. 213, Article ID 108305, 2022.

[11] L. Luo, J. Wang, S. Zhou, G. Lou, and J. Sun, "A broad learning-based state estimation method for power system," *Energy Reports*, vol. 8, no. 5, pp. 1227–1235, 2022.

[12] I. Táczi, B. Sinkovics, I. Vokony, and B. Hartmann, "The challenges of low voltage distribution system state estimation—an application oriented review," *Energies*, vol. 14, no. 17, p. 5363, 2021.

[13] S. Song, H. Xiong, Y. Lin, M. Huang, Z. Wei, and Z. Fang, "Robust three-phase state estimation for PV-Integrated unbalanced distribution systems," *Applied Energy*, vol. 322, p. 119427, 2022.

[14] G. Cheng, S. Song, Y. Lin, Q. Huang, X. Lin, and F. Wang, "Enhanced state estimation and bad data identification in active power distribution networks using photovoltaic power forecasting," *Electric Power Systems Research*, vol. 177, Article ID 105974, 2019.

[15] J. Zhang, T. Bi, and H. Liu, "Dynamic state estimation of a grid-connected converter of a renewable generation system using adaptive cubature Kalman filtering," *International Journal of Electrical Power & Energy Systems*, vol. 143, Article ID 108470, 2022.

[16] A. Monticelli, *State Estimation in Electric Power Systems: A Generalized Approach*, Springer, Berlin, Germany, 1999.

[17] G. Strang, *Introduction to Linear Algebra*, Wellesley-Cambridge Press, Wellesley, MA, USA, 5th edition, 2016.

[18] A. Abur and A. G. Exposito, *Power System State Estimation: Theory and Implementation*, CRC Press, Boca Raton, FL, USA, 2004.

[19] A. Mutanen, P. Järventausta, M. Kärenlampi, and P. Juuti, "Improving distribution network analysis with new amr-based load profiles," in *Proceedings of the 22nd International Conference and Exhibition on Electricity Distribution (CIRED 2013)*, Stockholm, Sweden, June 2013.

[20] H. A. R. Florez, D. Marujo, G. P. López, J. M. López-Lezama, and N. Muñoz-Galeano, "State estimation in electric power systems using an approach based on a weighted least squares non-linear programming modeling," *Electronics*, vol. 10, no. 20, p. 2560, 2021.

[21] M. A. Murray-Lasso, "Alternative methods of calculation of the pseudo inverse of a non-full-rank matrix," *Journal of Applied Research and Technology*, vol. 6, no. 3, 2008.

[22] I. Dokmanic and R. Gribonval, "Beyond moore-penrose part i: generalized inverses that minimize matrix norms," 2017, https://arxiv.org/abs/1706.08349.

[23] A. Ben-Israel and T. N. E. Greville, *Generalized Inverses: Theory and Applications*, Springer, Berlin, Germany, 2003.

[24] J. L. Stensby, "Analytical and computational methods: chapter six- minimum norm solution and the least-square-error problem," 2022, http://www.ece.uah.edu/courses/ee448/.

[25] G. B. Békési, L. Barancsuk, I. Táczi, and B. Hartmann, "Benchmarking various pseudo-measurement data generation Techniques in a low-voltage state estimation pilot environment," *Applied Sciences*, vol. 12, no. 6, p. 3187, 2022.

[26] B. Hartmann, L. Barancsuk, D. Kertész, B. Sinkovics, I. Táczi, and I. Vokony, "Development of a state estimator based modular toolset – specialties of low voltage operation," *CIGRÉ Centennial Conference*, vol. 2021, 2021.

[27] L. Thurner, A. Scheidler, F. Schäfer et al., “Pandapower—an open-source Python tool for convenient modeling, analysis, and optimization of electric power systems,” *IEEE Transactions on Power Systems*, vol. 33, no. 6, pp. 6510–6521, 2018.

[28] E. On, “Hungary synthetic load profiles,” 2022, https://www.eon.hu/hu/rolunk/vallalatcsoport/kozlemenyek/szabalyzatok-jogszabalyok/aram/eon-eszakdunantuliaramhalozati/elosztoi-szabalyzat-kizarolag-honlapon-publikalando-mellekletei.html.

[29] I. Táczi, I. Vokony, B. Hartmann, and G. M. Péter, “Low voltage state estimation based operation analysis of smart distribution assets,” in *Proceedings of the 2022 8th International Youth Conference on Energy (IYCE)*, Eger, Hungary, July 2022.

[30] M. Sojer, “Voltage regulating distribution transformers as new grid asset,” *Procedia Engineering*, vol. 202, pp. 109–120, 2017.